UDC 669 . 14 - 42 : 620 . 192 . 45

Technology

Development of Production Technologies of High-quality Special Steel for Bar and Wire Rod at Muroran Works

Ryoichi KAKIMOTO*
Michio NITTA
Shunji MIYAMOTO
Masato KOBAYASHI
Susumu KUDO
Mitsuhiro MATSUSHIMA
Taro HIROSUMI

Abstract

High-grade special steel for bar and wire rod manufactured at Muroran Works is used mainly for critical automotive parts, and quality measures such as the control of non-metallic inclusions and the surface layer structure are essential. Cost reduction based on stable operation is also important for improving competitiveness in the world market. As examples of such efforts, this paper presents some improvement measures taken in the essential processes for high-grade special steel, RH degassing, and continuous casting (CC). Frequent refractory problems of the lower degasser vessel and the snorkels have been greatly decreased by combining hot inspection and repair of the refractories, and consequently, steel quality has been improved and sequential processing increased, enhancing productivity. In the CC, the cooling pattern of the secondary cooling has been changed and the 3rd cooling modified for structure control, and thus, billet surface quality has been improved and the product yield remarkably enhanced.

1. Introduction

Muroran Works of Nippon Steel Corporation supplies a wide variety of steel materials for automotive parts such as springs, gears, and shafts; they account for 70% of all the products of the works (**Fig. 1**). In recent years, to compete with rapidly growing steelmakers in China and other Asian countries, it is essential to attain higher quality levels and further reduce costs. In order to remain competitive, in particular, in the market of middle- and high-grade products of high added value, it is important to maintain and continue to improve the quality of high-purity steels, for which fine control of nonmetallic inclusions and ultra-low oxygen content are required, typically such as those for automotive applications.

The manufacturing facilities of the Steelmaking Plant of Muroran Works comprise converters or basic oxygen furnaces (BOFs), a ladle furnace (LF) and a vacuum degasser (RH) for secondary refining, a continuous caster (CC), and a bloom rolling mill (**Fig. 2**). For the production of clean steel, extensive RH treatment is conducted to maintain and improve steel quality, but since extensive treatment

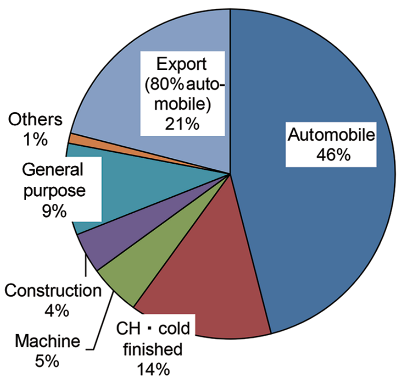

Fig. 1 Products of Muroran Works

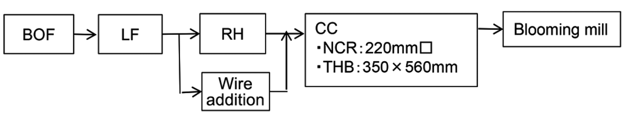

Fig. 2 Steelmaking processes of Muroran Works

* Senior Manager, Head of Dept., Steelmaking Technical Dept., Steelmaking Div., Muroran Works
12 Nakamachi, Muroran City, Hokkaido 050-8550

tends to inflict damage on the vacuum vessel refractories, operation problems occur frequently, and refractory maintenance has always been a heavy task. To solve the problem, an on-line hot inspection system for the refractories was introduced, and improvement measures using it were studied. In the CC process, a serious problem was that surface defects of blooms leading to rejection at product inspection occurred frequently especially with high-carbon steels. Measures were taken to solve the problem by improving the secondary cooling in the CC machine and the 3rd cooling before the bloom rolling.

2. Stable Production of Clean Steel by Stabilizing RH Operation

2.1 Outlines of measures

In the manufacture of clean steel, operation improvement of the RH degassing, which is the final steel refining process, has significant effects on the product quality. RH problems accounted for 68% of the rejects of clean steel products (**Fig. 3**), and 66% of these resulted from refractory problems (**Fig. 4**). RH refractory problems can be roughly divided into two types: the refractory mainly of the immersion pipes called the snorkels breaking and falling off[1]; and the steel vessel shell becoming red hot and through holes forming mainly in the lower vessel. It is feared that, when the refractory (consisting of oxide) falls off from the snorkel, it is mixed into molten steel, and when the vessel shell is red hot or a hole opens through it, the external atmosphere enters the vacuum vessel, leading to oxide formation and interruption of the processing. Maintaining the integrity of RH refractories, therefore, is essential for the production of clean steel of high added value. **Figure 5** shows the part names of an RH vessel. At Muroran Works, it is possible to melt and remove metal skulls on the vessel inner wall using a top oxygen lance at an off-line position. **Figure 6** shows the results of an investigation of refractory problems in the lower vessel and the snorkels and presumed causes. In the lower vessel, the refractory at the vessel bottom (the part in red in Fig. 6) is severely eroded, and the molten steel touches the steel shell, leading to the formation of a hole. Regarding the snorkels, it was presumed that rapid temperature rise at the start of the processing and temperature drop thereafter are repeated, and cracks formed and propagated in the refractory owing to the consequent expansion and contraction, leading to its breakage.

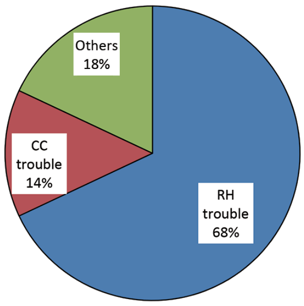

Fig. 3 Causes of rejects of clean steel

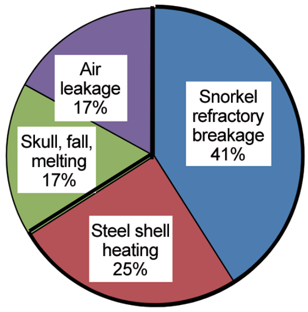

Fig. 4 RH troubles causing rejects of clean steel

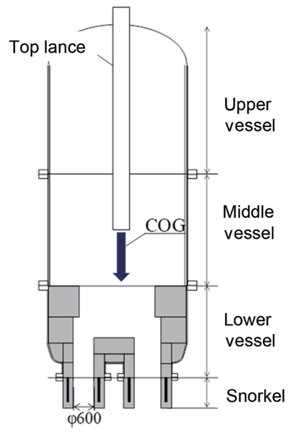

Fig. 5 Sectional view of RH vessel

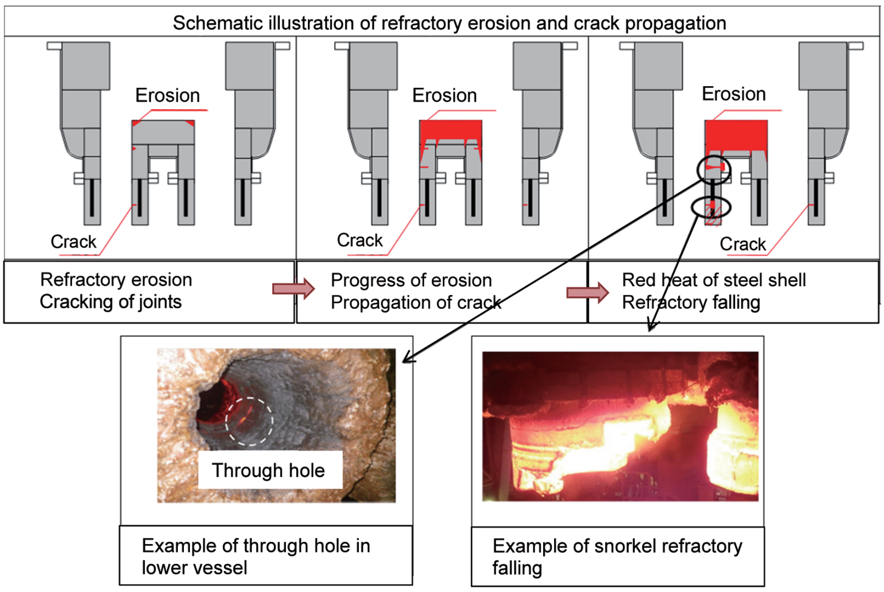

Fig. 6 RH refractory troubles and estimated causes

2.2 Introduction of RH online hot inspection equipment

Frequent and detailed inspections and appropriate repairs[2, 3] are necessary to prevent the above refractory problems, but by visual inspection from a safe place (diagonally below the RH vessel), it was impossible to obtain a detailed view of the problems, and repair work had to be decided based on insufficient information. Against this background, an inspection facility, called the RH online hot inspection device, was introduced for thorough refractory inspection in heat. The effect of the device to improve the repair method and its contribution to the production of clean steel are described below.

In the study of the inspection device, the following four points were considered: ensuring working safety, maintaining steel quality, improving operability, and cost reduction.

In particular, the following three points were emphasized:
(1) Automated remote operation;
(2) Wider temperature range of inspection; and
(3) Coverage of the entire circumference of the snorkels.

The system was organized as follows: images of the snorkels would be taken using cameras installed on swing arms to cover the inner walls and those to cover the outer walls, and the images would be processed by a computer in the operators' room and displayed on a monitor (**Fig. 7** (a)). To inspect the entire inner surfaces, three cameras were provided for each of the snorkels, and four other cameras separately provided to cover all the outer surface areas (Fig. 7 (b)). Each of the cameras were protected from falling objects, heat, and dust by a protective box with a lid and a window of heat-resistant glass (Fig. 7 (c)). The time required for the hot inspection of all the snorkel surface areas was set at roughly 70 s.

2.3 Clarification of mechanism of refractory problems

A cause of the RH refractory breakages is pitting due to the formation and growth of cracks. Accordingly, the occurrence and growth of cracks were investigated in detail using the RH online hot inspection device, and the cracks were found to grow significantly during the third and the seventh batches of sequential processing, and the following two characteristics were confirmed in common to both those batches.

- There was a large difference of refractory temperature between the end of the previous batch and the start of the batch in question.
- The waiting time between the batches was long.

The above indicates that cracks grow significantly when the

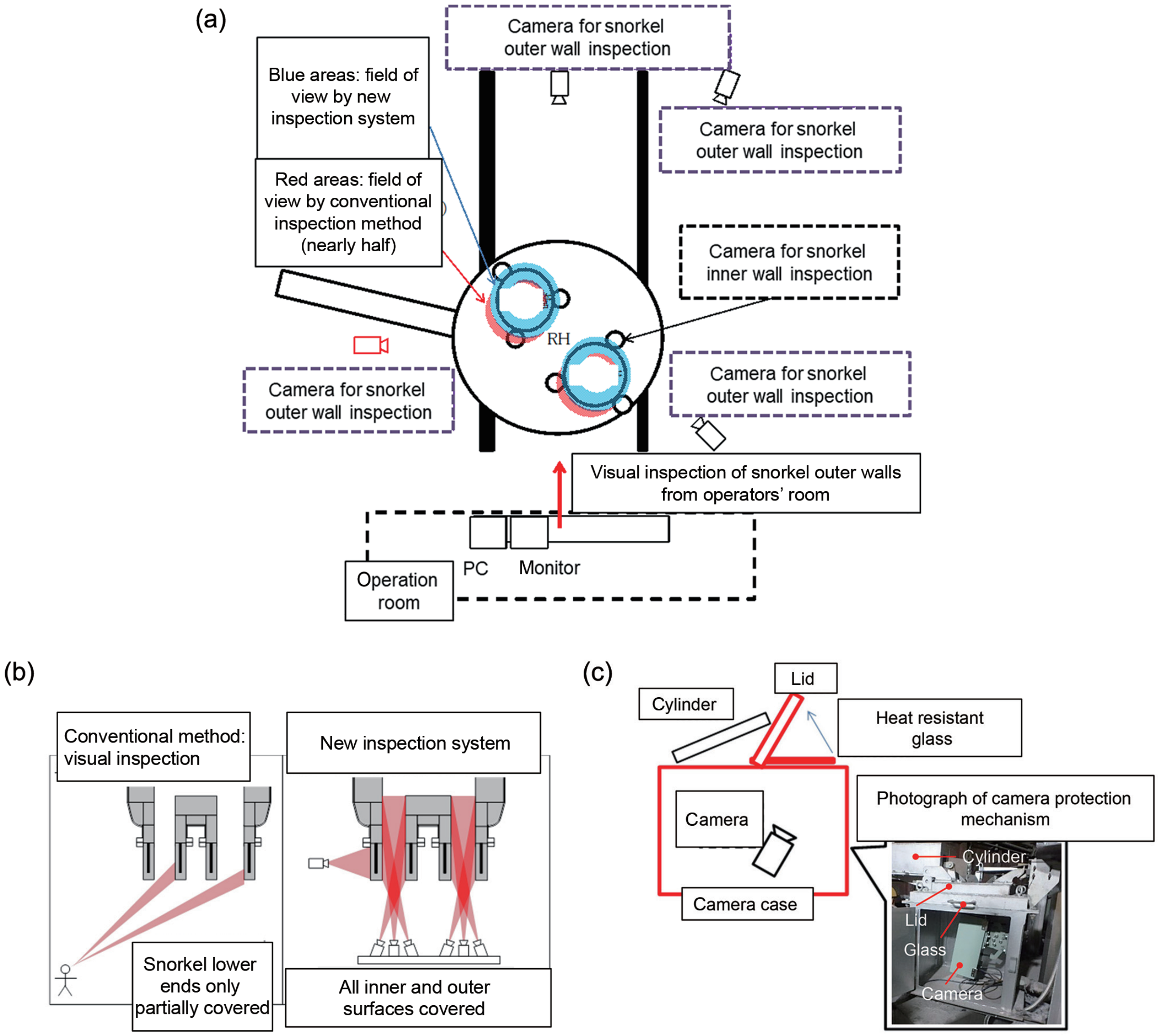

Fig. 7 RH online hot inspection system
(a) System arrangement, (b) Conventional and new inspection methods for snorkels, (c) Camera protection

temperature difference between the refractory surface and the molten steel is large. **Figure 8** shows the relationship between the crack growth rate and the temperature difference between the two. When the temperature difference exceeded 50°C, cracks began to extend, and the larger the temperature difference, the more they extended. **Figure 9** shows the result of analysis of crack depth and crack growth rate with and without spray repair. Based on the result, a repair standard was established as follows according to the crack depth index:

- Crack depth index ≤0.4: to be repaired by refractory spraying; crack growth is prevented nearly completely.
- Crack depth index >0.4: to be repaired by press-fitting of refractory; impossible to suppress crack growth by spraying.

As all the red-heating and the holes of the vessel shell occurred near the bottom, the progress of the erosion of the bottom refractory was observed, and it was found that when the skulls on the vessel inner wall were melted by the top oxygen blowing, the erosion advanced exponentially with the blowing time. As a countermeasure, the frequency of skull melting by the top blowing was increased and the time of each blowing was shortened to roughly 45 min, and the occurrence of the refractory problems in the lower vessel decreased to 0.2% or less (**Fig. 10**).

2.4 Effects of RH online hot inspection system

Figure 11 shows the change of the RH refractory problems before and after the introduction of the hot inspection system. No refractory problems have occurred since it was introduced. Due to the absence of sudden refractory problems, the service life of the lower vessel has been extended to the above planned figure (**Fig. 12**). The reject ratio of clean steel decreased by roughly 10% from that in the fiscal year 2015 (ending in Mar. 2016, see **Fig. 13**), and the number of sequential processing increased by four batches on average from that when a smaller number of sequential batches had been set as the standard as a precaution against the refractory problems.

2.5 Summary of measures against RH refractory problems

Significant damage to the refractories occurred frequently in the manufacture of high-grade special steel of a high added value for bars and wire rods. To minimize the problems of RH refractory, the RH online hot inspection system was introduced, the cause of the problems was investigated, measures were taken against them, and the following results were obtained.

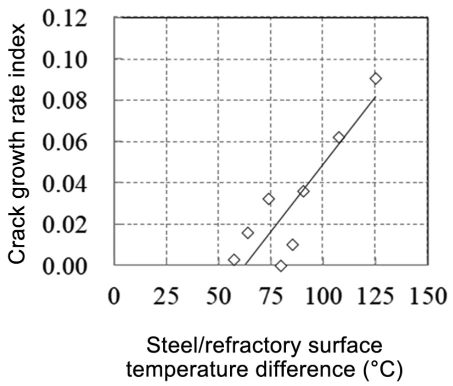

Fig. 8 Relationship between steel/refractory surface temperature difference and crack growth rate

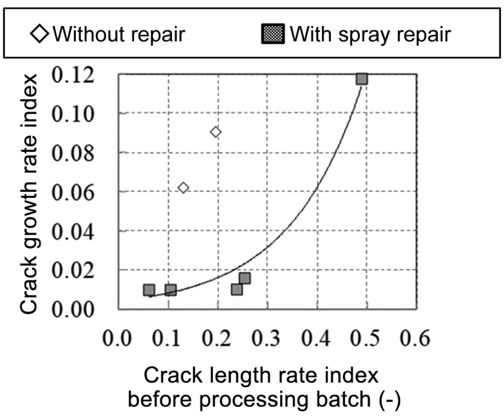

Fig. 9 Change in crack growth rate with and without spray repair (temp. difference between refractory surface and steel = 100°C ± 20°C)

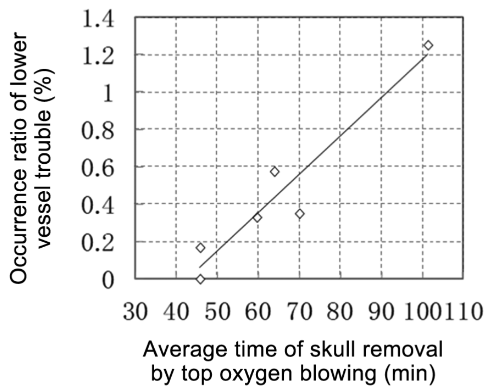

Fig. 10 Relationship between top oxygen blowing time and occurrence of lower vessel refractory troubles

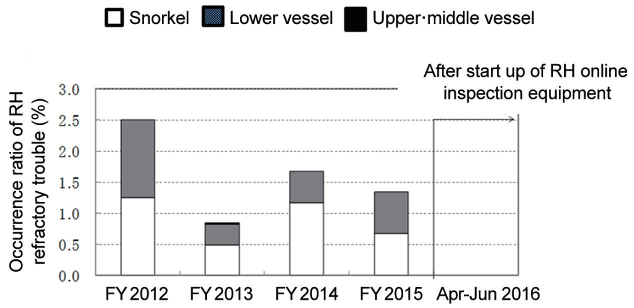

Fig. 11 Change in RH refractory trouble occurrence ratio

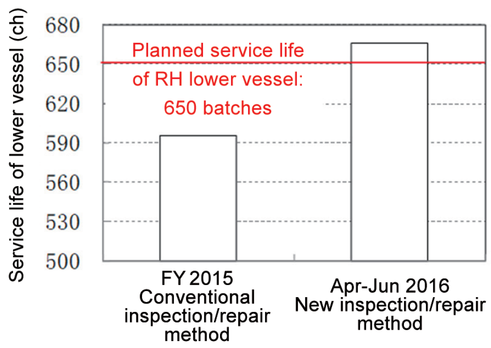

Fig. 12 Change in lower vessel service life

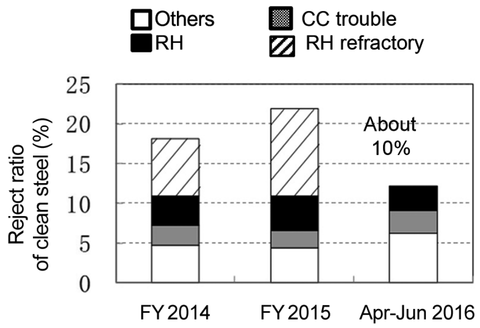

Fig. 13 Rejects of clean steel by cause

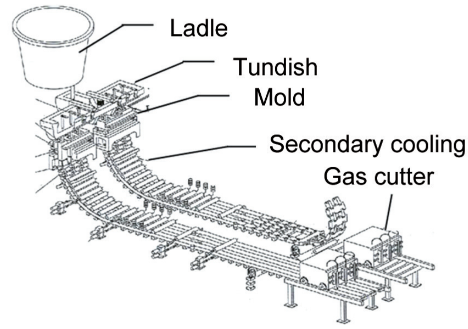

Fig. 14 Overview of continuous caster

1) By the RH online hot inspection system, inspection of the inner and outer surfaces of the snorkels in the entire circumference and the lower vessel has been enabled.
2) The following three improvements have been implemented in the equipment inspection between the processing batches:
 • Working safety: it has become possible to conduct all equipment inspection work in the operators' room.
 • Inspection time: the inspection time has decreased from 9 to 3 min, approximately.
 • Pre-heating time: to better protect the refractories, sufficient reheating time has been secured thanks to the shortened equipment inspection time.
3) The problems of the RH refractory breakage and red heating and through holes of the vessel shell were investigated, and the following findings were obtained:
 • The cause of the refractory breakage was cracks originating from the surface and growing as the temperature difference increased between the refractory surface and the molten steel increased. The crack growth has been suppressed by spraying of refractory. It has to be noted, however, that the effect of the spray repair differs depending on the crack depth as given below.

Crack depth	Spray repair effect	Repair method
Crack depth index ≤ 0.4	Suppress crack growth	Refractory spray
Crack depth index > 0.4	Impossible to suppress crack growth	Refractory press fitting at early stage of crack growth

 • The red heating and through holes of the vessel shell resulted from the thinning by the erosion of the vessel bottom refractory, which advanced during the vacuum processing, and remarkably especially during skull melting by the top oxygen blowing. By limiting the top blowing time to 45 min or less, the occurrence of lower vessel problems has been lowered to 0.2% or less.
4) As a result of 1) to 3) above, the reject ratio at steel quality inspection has been decreased by 10%, and the number of sequential processing increased by four batches.

3. Improvement of Surface Quality of Medium-section Blooms

3.1 No. 3 CC-bloom polling process and occurrence of defects

Figure 14 shows an overview of No. 3 CC, which required improvements. It casts six blooms, each 220×220 mm in sectional size, simultaneously in two strands, each comprising three streams.

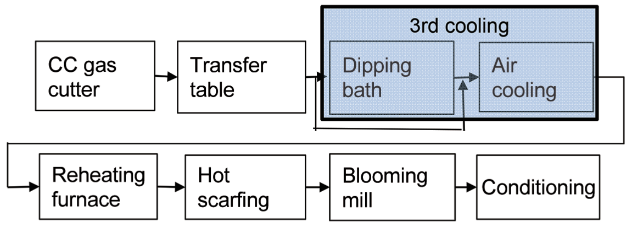

Fig. 15 Flow of NCR process after CC

This process is internally referred to as the NCR process standing for near net shape casting and compact high reduction. **Figure 15** shows the process flow from the exit of No. 3 CC to the bloom rolling. To prevent grain boundary cracking during bloom rolling, 3rd cooling is applied to the cast blooms in two alternative routes: air cooling with and without prior water immersion cooling in a dipping bath (hereinafter referred to as the DB).

Surface defects appeared in the billets after the bloom rolling, and their occurrence frequency differed depending on the carbon content of the steel. **Figure 16** shows the defect occurrence of different steel grades; as seen here, high-carbon steel accounted for nearly 50% of the total. Improvement measures were taken against these defects. **Figure 17** shows the types of defects seen with high-carbon steel, and the occurrence ratios. The surface defects of high-carbon steel are roughly classified into two types: micro cracks and longitudinal cracks. **Figure 18** shows the results of a detailed investigation of a hole and a longitudinal crack, and the casting speed (Vc) of the blooms from which the defected billets were rolled.

3.2 Measures against micro cracks

3.2.1 Inference of micro crack forming mechanism

Table 1 shows the chemical composition of a typical steel grade prone to the micro cracks. Such depressions are most likely to occur with high-carbon, high-nitrogen steel, and more frequently on the upper face (hereinafter referred to as the L face) of original blooms than on the others. As a result of a microstructural observation of the hole, although there was no solidification disorder or abnormal solidification structure, a decarburized layer was confirmed to exist at the site of the hole, and it was considered to have formed somewhere from the CC machine to the reheating furnace before the blooming mill. To find the cause of the holes, the surfaces of as-cast blooms of the steel grades prone to this type of defect were inspected, and cracks were found on the L face. **Figure 19** shows a crack, and **Fig. 20** its sectional photomicrograph.

As seen in Fig. 20, it has sharp edges suggesting that it originated from an α phase deposited at a prior γ grain boundary. It was presumed from this that the crack grew deeper along the grain bound-

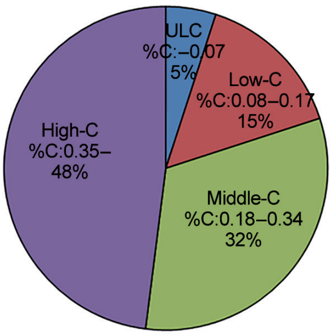

Fig. 16 Occurrence of surface defects by carbon content in steel

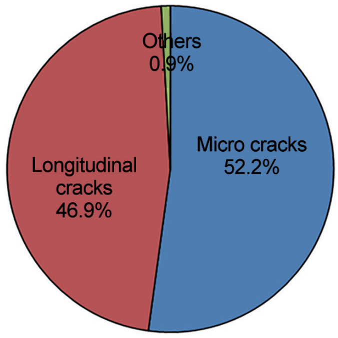

Fig. 17 Types of surface defects of high-carbon steel

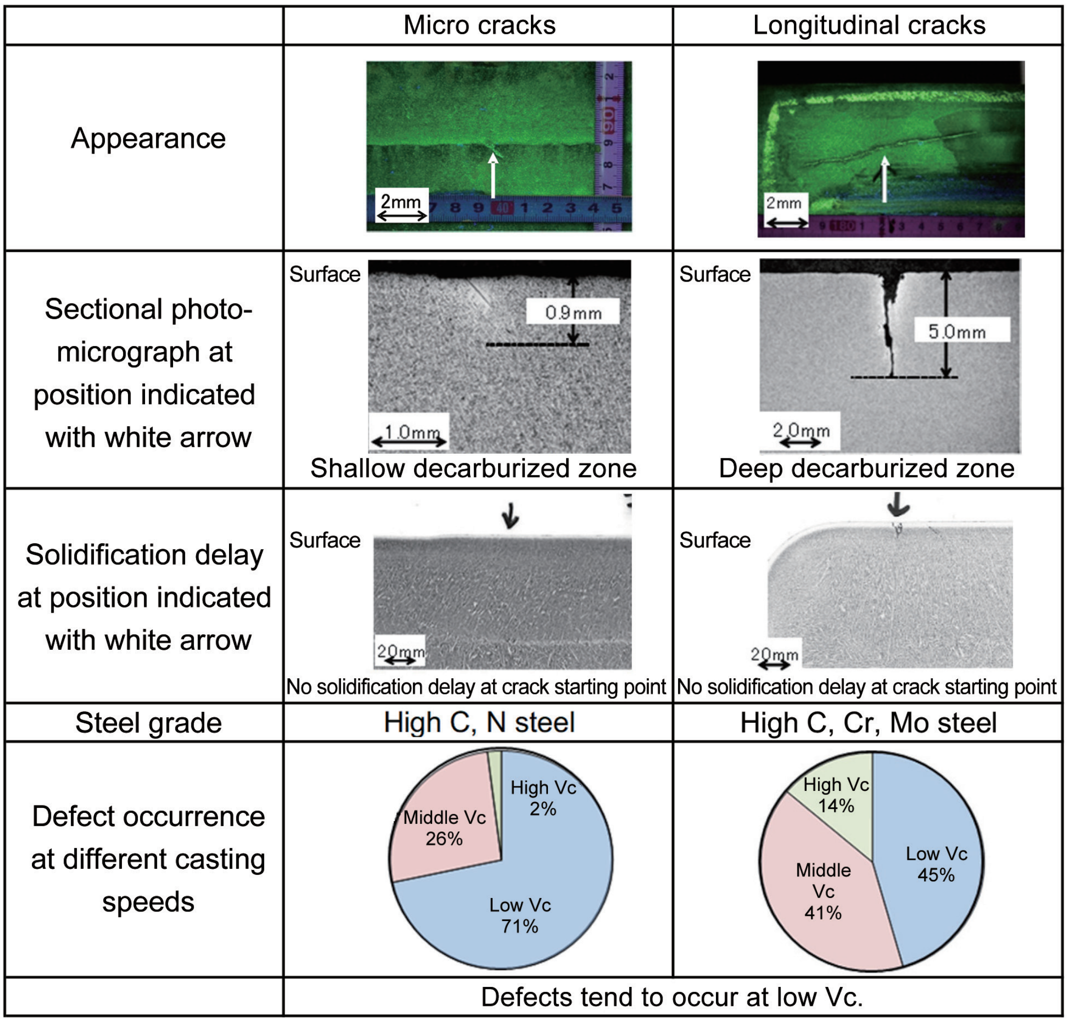

Fig. 18 Characteristics of surface defects occurring in high carbon steel

ary during the bloom rolling to become a hole. It was presumed also that the crack serving as a starting point of a hole formed because force exceeding the limit strain was applied on the L surface layer of the cast bloom at the unbending point of the CC, where strain is imposed on the L side, and grain boundaries embrittle. According to Suzuki et al.,[4, 5] this embrittlement of cast blooms is grain boundary embrittlement due to precipitates such as Nb(C·N), AlN, and BN at γ grain boundaries, and films of proeutectoid ferrite depositing there.

3.2.2 Study of conditions for preventing micro cracks

Figure 21 shows the results of the Greeble test of high-carbon, high-nitrogen steel. The lowest bloom temperature at which no cracking occurs at the CC unbending point was estimated, and it was found that blooms would embrittle at 900°C or below. By the NCR process, the bloom temperature is lower at the corners than at

Table 1 Chemical composition of typical steel in which micro cracks occur frequently

Steel grade	%C	%Si	%Mn	%V	N ppm
High C, N	0.43	0.25	1.37	0.087	92

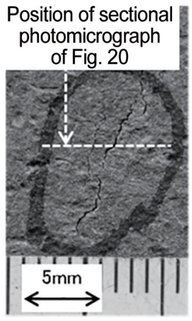

Fig. 19 Appearance of bloom L face at position corresponding to micro crack of billet

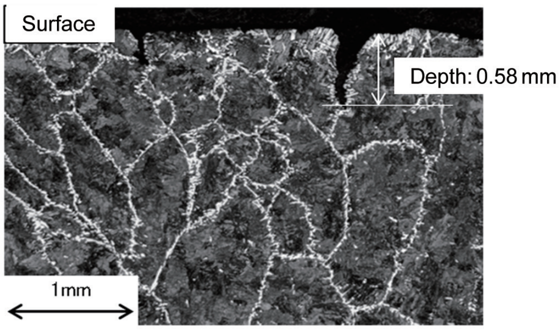

Fig. 20 Sectional photomicrograph of crack (nital etched)

face centers by about 80°C owing to the cooling from two sides. It follows therefore that, in order to prevent the occurrence of the holes, it is necessary to keep the bloom temperature at the corners at 900°C or higher, which means 980°C or higher at the L face center, at the unbending point. Development of a new secondary cooling pattern of the caster to bring about this condition was started.

3.2.3 Development of new secondary cooling pattern

1) Design of new secondary cooling pattern of variable specific water ratio

Table 2 shows the specific water ratios for different secondary cooling patterns and casting speeds (Vc), and evaluation of their applicability; the developed new pattern is evaluated based on calculation. The conventional secondary cooling patterns were designed so that the specific water ratio remained unchanged regardless of Vc. However, when the specific water ratio is kept unchanged, the bloom temperature changes depending on Vc because of the difference in the heat removal by the rolls. For this reason, aiming both at higher bloom temperature at the machine end and lower equipment load, the new pattern was designed so that, at high Vc, the specific water ratio would be the same as that for the normal cooling by the conventional pattern, and at low Vc, the same as that for ultra-slow cooling.

2) Result of application of new pattern to actual production

After applying the new pattern, the machine inside ambient temperature near roll bearings was lowered to well below a target temperature of 200°C. On the other hand, **Fig. 22** compares the temperature at the L face center of blooms cast at low Vc applying different secondary cooling patterns, measured at the unbending point. By applying the new pattern, the bloom temperature has risen by 20°C from that by the conventional pattern, clearing the target temperature of 980°C. **Figure 23** compares the occurrence of the micro cracks before and after the application of the new pattern. It was confirmed that by applying the new pattern the occurrence of the micro cracks decreased by 93%.

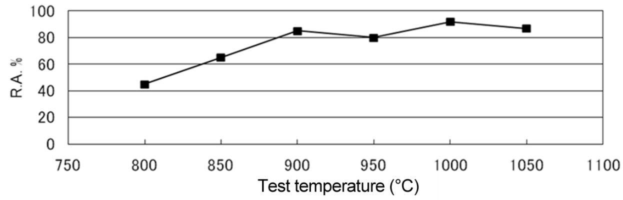

Fig. 21 Relationship between temperature and reduction of area by Greeble test

Table 2 Specific water ratios for different secondary cooling patterns and evaluation of applicability vis-à-vis objectives

	Cooling pattern	Conventional: Normal cooling	Conventional: Ultra-slow cooling	New cooling pattern
Specific water ratio	High Vc	Large	**Small**	**Large**
	Low Vc	**Large**	Small	**Small**

Objectives	Cooling pattern	Normal cooling	Ultra-slow cooling	New cooling pattern
Lowering machine load: Machine inside air temp. near roll bearings ≤ 200°C	High Vc	Good	Poor	Good
	Low Vc	Good	Good	Good
Higher bloom temp.: L face center at unbending point ≥ 980°C	High Vc	Good	Good	Good
	Low Vc	Poor	Good	Good

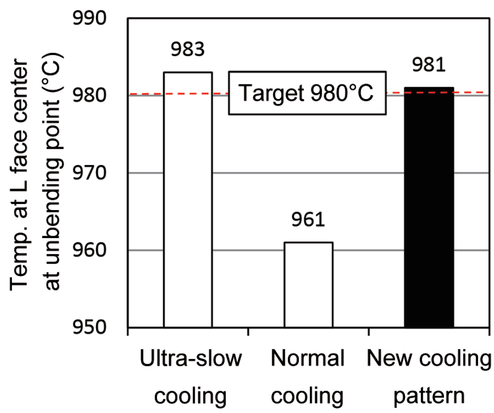

Fig. 22 Temp. of L face center at unbending point by new cooling pattern

3.3 Measures against longitudinal cracks

3.3.1 Inference of longitudinal crack forming mechanism

Table 3 shows the chemical composition of a typical steel grade prone to the longitudinal cracks. The explanation below focuses on high-carbon Cr-Mo steel, in which they are most likely to occur. The surface appearance of a longitudinal crack and its sectional photomicrograph are given in the right-hand column of Fig. 18. The cracks stretch in the direction of casting, are comparatively deep, roughly 1.5 to 5.0 mm, occur under conditions where decarburization is likely to proceed, and at certain bloom faces than at others. **Figure 24** shows the arrangement of the strands and streams of the caster, and the names of the bloom faces; the incidence of the cracks tends to be high at the faces in opposition to another stream (hereinafter referred to as the inner faces).

No external force is applied to the side faces of the blooms in the route from the CC machine to the reheating furnace, and it was estimated that the longitudinal cracks were caused by internal strain due to the thermal expansion and contraction of the bloom itself. To investigate the temperature history of the bloom, the bloom surface structure after the cooling in the DB was examined. **Figure 25** shows photomicrographs of the solidification structure at a bloom face not in opposition to another stream (hereinafter referred to as the outer face; all L and F faces are the outer faces) and that at an inner face. The steel grade of the specimen is that given in Table 3, and it was cast at a low Vc. The surface structure of the outer face after the DB cooling consisted of an α+P phase. At the inner face, in contrast, the α+P phase alone was present only within 1 mm from the surface, and deeper inside, the structure was different with sites of martensitic transformation.

Figure 26 schematically shows the mechanism of the formation of longitudinal cracks. The crack formed presumably after the DB cooling owing to the structural difference between the faces. From the fact that martensitic transformation occurred at depths of more than 1 mm of the inner faces, it was assumed that the transformation sites were in an untransformed γ structure before the DB cooling, and martensitic transformation was caused by the cooling. It was assumed that a tensile stress was created at the transformation sites owing to the transformation expansion, those sites served as the starting points of the cracks, and thus, cracks 1 mm or more in depth formed at the inner faces.

Figure 27 shows the continuous cooling transformation (CCT) curve of the steel grade in Table 3 during cooling at a rate of −0.1°C/s, equivalent to the cooling rate in the CC. The bloom temperature just before the DB cooling varies from face to face: 615 to 635°C at the inner faces and around 600°C at the outer faces. Figure 27 confirms that before the DB, the outer faces are at roughly 600°C, nearly equal to the Ar1 point, and that the immersion cooling is applied after cooling to a temperature range in which the α+P transformation is completed. From another fact that the structure after the DB is completely in the α+P phase, it is presumed that the α+P transformation was completed before the DB cooling.

At the inner faces, in contrast, the temperature before the DB is 615 to 635°C, lower than the Ar3 point and higher than the Ar1 point. This indicates that the immersion cooling was commenced after the α+P transformation had started, but at that time untrans-

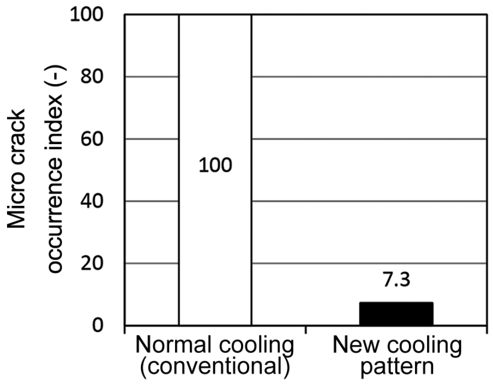

Fig. 23 Decrease of micro cracks by new cooling pattern

Table 3 Chemical composition of typical steel in which longitudinal cracks occur frequently

Steel grade	%C	%Si	%Mn	%Cr	%Mo
High C, Cr, Mo	0.41	0.24	0.78	1.115	0.116

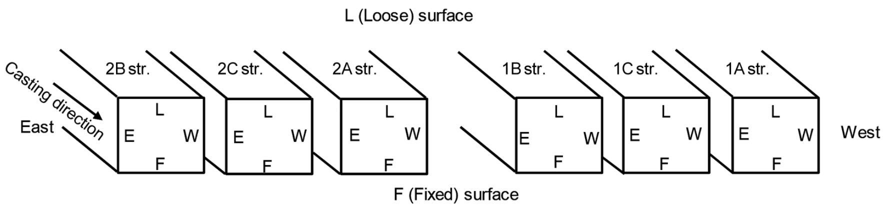

Fig. 24 Arrangement of CC strands/streams and names of bloom faces

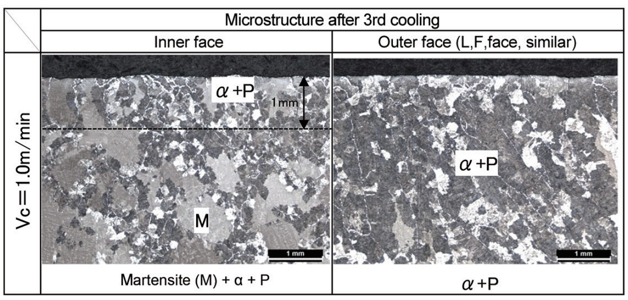

Fig. 25 Microstructure of bloom surface layer after 3rd cooling

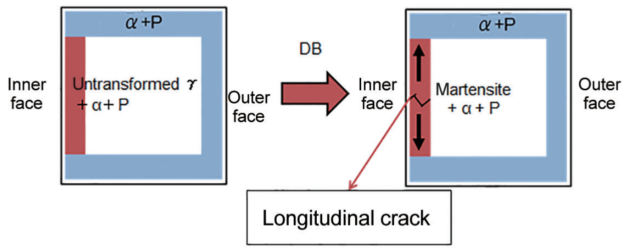

Fig. 26 Schematic illustration of occurrence of longitudinal cracks

formed γ structure remained locally. In addition, since the structure after the DB cooling is in the martensite+α+P phase, it is presumed that the α + P transformation was completed locally before the DB, but untransformed γ remained, which then transformed into martensite during the DB cooling. Based on these assumptions, the proposed mechanism of the longitudinal crack formation given in Fig. 26 is considered appropriate.

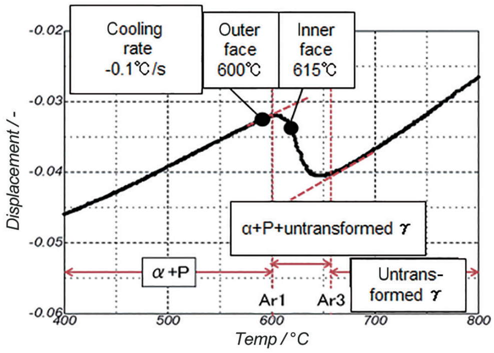

Fig. 27 CCT curve of steel in which longitudinal cracks occur

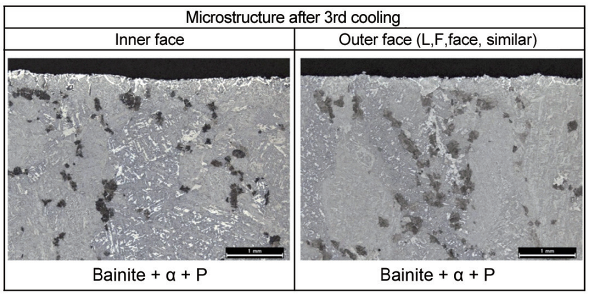

Fig. 28 Microstructure of bloom surface layer after 3rd cooling (high Vc)

On the other hand, **Fig. 28** shows photomicrographs of the surface structure of the outer and inner faces after the DB, the bloom being cast at high Vc, and **Fig. 29** the CCT curve of the steel. When Vc is high, transformation into a bainite+α+P phase occurs at all the faces, and consequently, there is no difference in the surface structure, no martensitic transformation takes place, and for this reason, no longitudinal cracks are expected to form. This is presumably because the water cooling in the DB was applied when the bloom temperature was as high as shown in Fig. 29, and the blooms were not cooled to the starting temperature of martensitic transformation.

3.3.2 Measures against longitudinal cracks

Figure 30 shows the cause of longitudinal cracks and countermeasures against them. Of the countermeasures studied, application of air cooling to the 3rd cooling is explained below. In the study of the countermeasures, it was presumed as follows: when Vc was low, the blooms would be cooled such that the α+P transformation was completed near the surfaces, and the untransformed γ remained only in the bloom inside; the DB cooling of the bloom in this condition causes the formation of longitudinal cracks; and they could be prevented from forming by applying air cooling to the 3rd cooling so that untransformed γ would not change into martensite, and all surface layers would be transformed completely into the α+P phase. **Figure 31** shows the CCT curve during the 3rd cooling totally by air cooling before the charging into the reheating furnace. The graph shows that all the bloom surfaces are air-cooled to below the Ar1 point, and the bloom is charged into the reheating furnace after the transformation into the α+P phase is completed at all the faces. In this case, longitudinal cracks are prevented from forming.

Figure 32 compares the occurrence of the longitudinal cracks in the steel grades prone to them before and after the above change in the 3rd cooling. The occurrence of the longitudinal cracks was decreased by 74% by applying air cooling alone to the 3rd cooling.

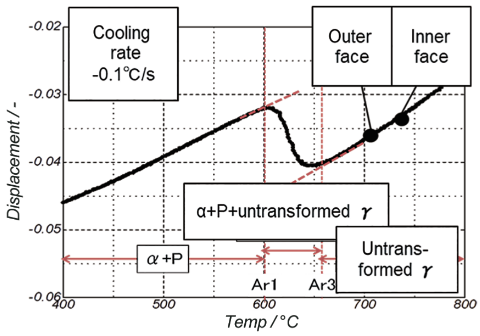

Fig. 29 CCT curve of steel in which longitudinal cracks occur (high Vc)

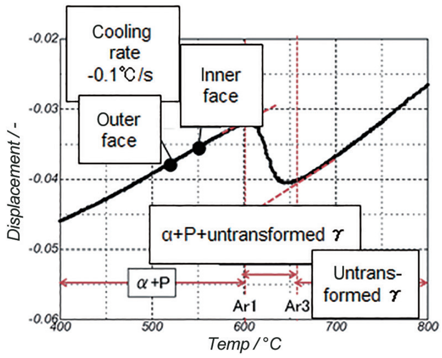

Fig. 31 CCT curve and temp. during air cooling

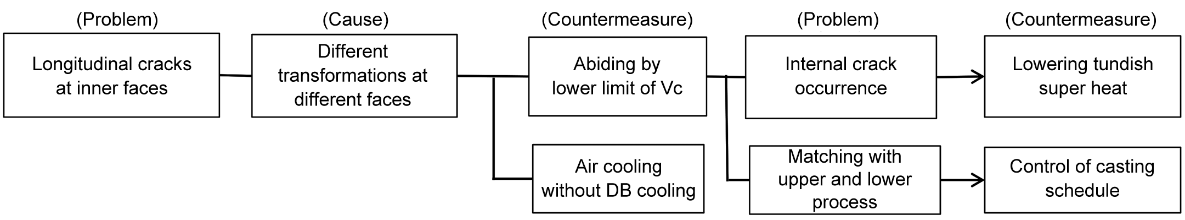

Fig. 30 Cause of longitudinal cracks and countermeasures

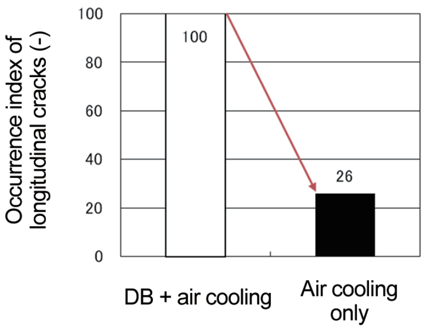

Fig. 32 Decrease of longitudinal cracks by elimination of DB cooling

3.4 Summary of measures against billet surface defects

The following improvement measures were taken against typical billet surface defects of the NCR process.

1) The formation mechanism of micro crack defects was specified, and as a countermeasure, a new secondary cooling pattern has been applied to the CC operation, by which virtually the same bloom temperature as that by the conventional ultra-slow cooling pattern has been realized in a low Vc range, and as a result, the occurrence of the micro cracks has fallen by 93%.
2) As a countermeasure against longitudinal cracks, air cooling has been applied to the 3rd cooling of cast blooms, and consequently the occurrence of the cracks has decreased by 74%.

4. Conclusion

This paper has presented the measures to improve the productivity of high-grade special steel for bars and wire rods manufactured at Muroran Works, the measures to avoid processing problems of the RH degasser, and those to minimize surface defects of CC blooms. As a result of those measures, the defects have been remarkably decreased and the product reject ratio has been significantly improved.

References

1) Matsunaga, H., Tominaga, T., Ohji, M., Tanaka, H.: Tetsu-to-Hagané. 63 (13), 1945–1952 (1943)
2) Itou, S., Inuzuka, T.: Shinnittetsu Giho. (388), 65–67 (2008)
3) Inuzuka, T., Kojima, A., Kataoka, K., Sakamoto, K.: Taikabutsu. 50, 492–493 (1998)
4) Suzuki, H., Nishimura, T., Yamaguchi, S.: Tetsu-to-Hagané. 65 (14), 2038–2046 (1979)
5) Suzuki, H., Nakamura, Y.: J. of Japan Institute of Metals and Materials. 18 (11), 748–754 (1979)


Ryoichi KAKIMOTO
Senior Manager, Head of Dept.
Steelmaking Technical Dept., Steelmaking Div.
Muroran Works
12 Nakamachi, Muroran City, Hokkaido 050-8550


Susumu KUDO
Manager
Safety and Health Dept.
General Administration Div.
Muroran Works

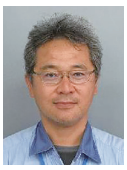
Michio NITTA
Senior Manager
Refractory Engineering Dept.
Refractory Ceramics Div.
Plant Engineering and Facility Management Center


Mitsuhiro MATSUSHIMA
Manager, Head of Section
Continuous Casting Section
Steelmaking Plant, Steelmaking Div.
Muroran Works


Shunji MIYAMOTO
Steelmaking Technical Dept.
Steelmaking Div.
Muroran Works

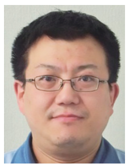
Taro HIROSUMI
Senior Researcher
Steelmaking Research Lab.
Process Research Laboratories


Masato KOBAYASHI
General Manager, Head of Div.
Steelmaking Div.
Muroran Works